Geophys. J. R. astr. Soc. (1977) 50, 333–352

Two-dimensional magnetotelluric inversion

GL03726

David L. B. Jupp* and K. Vozoff *School of Earth Sciences, Macquarie University, North Ryde, New South Wales 2113, Australia*

Received 1976 September 13

Summary. When complex structure is encountered in magnetotelluric surveys, interpretation by locally fitted layered models is of questionable validity. However, when the processed data show two-dimensional structure, numerical inversion schemes for two-dimensional models may be constructed as an aid to regional data interpretation.

The two-dimensional magnetotellurics inversion problem is here formulated in a way that may be applied to many problems. A resulting computer program is analysed carefully in terms of its cost relative to that of simpler layered modelling.

As an example, the method is applied to some field data where the interpretive advantages of the program become evident.

1 Introduction

1.1 MODELLING MT TRAVERSE DATA

Magnetotelluric (MT in the following) data in the forms of apparent resistivity, phase and Tipper measurements ('Earth Response Functions', or ERF's as in Vozoff (1972) can be numerically modelled, and therefore in principle inverted, by various simplified structures. In Jupp & Vozoff (1975), and Vozoff & Jupp (1975), a general approach to numerical inversion is illustrated by modelling single site MT data with layered earth structure. These very simple models have commonly been used for MT interpretation (Patrick & Bostick 1969; Wu 1968; Vozoff 1972) as well as for the interpretation of other data as in Inman, Ryu & Ward (1973), and Glenn *et al.* (1973). When regional structure is approximately horizontal, as is the case in many sedimentary basins, and lateral variation is slow, good regional interpretations can be made by fitting layered earth models locally at MT sites, and patching the results together along the data traverses (Vozoff 1972). However, when structure is not approximately layered, fitting layered models involves systematic errors, and quantitative interpretation of the resulting regional models is very difficult. Examples of the distortion produced are given in Vozoff *et al.* (1975), although the example presented here in Section (3.3) shows how local layered modelling can provide useful qualitative information.

* Present address: CSIRO Division of Land Use Research, PO Box 1666, Canberra City, ACT, 2601, Australia.

A more general structure that can be modelled is two-dimensional (or 2D) structure, in which regional conductivity varies little in one direction (the 'strike' direction), and where data are collected approximately across strike. 2D structures have been numerically modelled by various methods. For example, Neves (1957), and Jones & Price (1970) have used classical finite differences (although the discussions by Williamson, Hewlett & Tammemagi (1974), and Jones & Thomson (1974) should be noted), while Swift (1967, 1971) and Madden & Swift (1969) use difference schemes based on a network analogy (see Praus (1975) for a review). Other methods, such as the Finite Element Method (Coggan 1971 and Rodi 1976) and the Integral Equation methods of Hohmann (1971) and Lee (1975) have been used for 2D electromagnetic modelling, and may provide useful bases for 2D or even 3D (Hohmann 1973) inversion. All of these methods can lead, in principle, to numerical inversion schemes, ranging from crude search by trial and error, to more sophisticated schemes using partial derivatives. Weidelt (1975) has made good progress using the Integral Equation Method for the inverse Geomagnetic Depth Sounding problem, and Ku (1976) has used the network method for the inversion of a somewhat restricted MT data set.

In the following, a finite difference modelling method is used, and partial derivatives evaluated for it. Much the same approach could be used with any of the methods mentioned, and with various geophysical ERF's.

Any such method must, however, face the problems that arise from the significant growth in computing cost associated with 2D inversion. In economic terms, computing cost varies widely depending on the given situation, so that cost in the present context is relative in the sense that 2D inversion might be 10 times more costly than layered interpretations on the same data. In terms of total economic cost of data collection and processing, such expense may not be unwarranted.

When times are quoted to indicate computing cost they are measured on a Univac 1106 time shared computer, with 256k memory, and EXEC 8 software. The times are about twice those expected if the program were run on a Univac 1108.

1.2 NUMERICAL INVERSION METHODS

The passage from simple layered model inversion to 2D inversion presents a significant change of scale, with respect to both the resulting interpretation, and the computing effort required to achieve it.

In Section 3, it is emphasized that both the data presented for inversion, and the initial model, should be the result of considerable care in order to justify the cost of MT 2D inversion. Assuming such care, the inversion method itself must be very efficient.

The methods used here are those described in Jupp & Vozoff (1975), and require partial derivatives of the model data with respect to the model parameters (or simply 'partials'). The solution methods are variants of the Gauss method (*cf.* Marquardt 1970) and use the Singular Value Decomposition (Lanczos 1960) of the Jacobian, or Matrix of partials, to iterate from an initial model, to one which fits the data within the limitations described in Jupp & Vozoff (1975). Important properties of the methods are their stability, and ability to converge in relatively few iterations.

The inversion concept behind our approach is one of interactive modelling or 'refinement modelling' (Anderssen 1975). That is, inversion as an aid to interpretation which improves the interpreters ideas of regional structure against the collected data. Backus & Gilbert (1967, 1968, 1970) (whose methods make an interesting comparison with the early paper by Golomb & Weinberger 1959), and Anderssen (1975), look for much more in their inversion

schemes. Their aim is to find generalized profiles without assuming special structures, and restricted model features. While that aim is important, the approach taken here is more pragmatic in that interpretation is attempted in terms of specific geological features, and practical in that the high cost of 2D inversion rules out extensive 'Non-uniqueness' modelling (Anderssen, Worthington & Cleary 1972).

The cost factor also handicaps attempts at 2D inversion that use 'Trial and error' (e.g. Swift 1967), or which are based on forward evaluations alone (e.g. Ku 1976). In this situation, the evaluation of partial derivatives for special models leads to relatively cheap, highly effective, and rapidly converging iterative schemes. It is worth pointing out, as was done by Glenn *et al.* (1973) for layered modelling, that approximations to partials by differencing also have very poor numerical properties, particularly near to a solution.

Even when inversion is not intended, the relatively low extra cost of partials evaluation allows important studies in the nature of superior 'parametric study' and experiment design to be made for 2D models as was done in Vozoff & Jupp (1977) for layered situations. These linearized studies, while not as general in their scope as non-uniqueness modelling (Anderssen 1975) can provide strong conclusions about model situations as shown in Section 3.3.

2 Numerical methods for MT 2D modelling

2.1 FORWARD MODELLING

The conventional right-handed Cartesian system, with z down, and y as the 'strike' direction along which conductivity does not vary, is assumed for coordinates. Maxwell's equations with a plane wave source then separate into two independent systems of partial differential equations, which are often referred to as the E-perpendicular (E-perp), and H-perpendicular (H-perp) to strike polarizations. The two systems may be written in the convenient common form,

$$LV = 0 \tag{2.1}$$

$$I_x = -MV \tag{2.2}$$

and

$$I_z = -NV \tag{2.3}$$

where the differential operators L, M, and N are defined by

$$M = \frac{1}{Z_x}\frac{\partial}{\partial x}$$

$$N = \frac{1}{Z_z}\frac{\partial}{\partial z}$$

$$L = -\frac{\partial}{\partial x}M + \frac{\partial}{\partial z}N + Y.$$

The functions V, I_x, I_z, Z_x, Z_z and Y are identified for each polarization as follows (*cf.* Madden & Swift 1969)

(i) E-perp to strike

$$V = H_y,\ I_x = -E_z,\ I_z = E_x,\ Z_x = Z_z = \sigma - i\epsilon\omega$$

and $Y = -i\omega\mu$

(ii) H-perp to strike

$$V = E_y,\ I_x = H_z,\ I_z = H_x,\ Z_x = Z_z = -i\omega\mu$$

and $Y = \sigma - i\epsilon\omega$.

The E and H terms are the electric and magnetic field components, ω is 2π frequency, σ is conductivity, which is a function of x and z only, and ϵ and μ are the permeability and susceptibility functions, which are assumed to be constant at the air and free space values ϵ_0 and μ_0.

This general form for the basic equations is adopted from the 'network' analogy due to T. R. Madden (Swift 1967, 1971; Madden & Swift 1969). The network method can be generalized into a comprehensive approach to numerical and analogue modelling for a broad class of geophysical problems (Madden 1972).

The usual ERF's for the MT method are defined from the solutions to the equations by

(i) E-perp to strike

$$\rho_{xy} = \frac{1}{\omega\mu}|Z_{xy}|^2 \qquad \phi_{xy} = \text{phase}\,(Z_{xy})$$

where $Z_{xy} = E_x/H_y$

(ii) H-perp to strike

$$\rho_{yx} = \frac{1}{\omega\mu}|Z_{yx}|^2 \qquad \phi_{yx} = \text{phase}\,(Z_{yx})$$

where $Z_{yx} = E_y/H_x$.

As well, the very important 'Tipper' (Vozoff 1972), or vertical to horizontal field ratio can be computed for the H-perp polarization as H_z/H_x. This ERF is related to the 'Parkinson Vectors', (Parkinson 1959) and to the general class of ERF's described by Lilley (Lilley 1974) for the geomagnetic induction problem.

In each case equation (2.1) is solved for V, I_x and I_z are generated from (2.2) and (2.3), and the appropriate ERF's computed by identifying components. It is important to notice, however, (Swift 1971) that the boundary conditions are not the same for both polarizations. For each case they are that the fields decay to zero in the earth, and that H_x and H_z are constant at the 'top' of the atmosphere. For E-perp, this means that V is constant, and for H-perp, that $\partial V/\partial z$ is constant at the 'top'.

To reduce (2.1) to a discrete system of equations by finite differences, one of a number of discretizations has been chosen. For example, Praus (1974) discusses the interesting variations in schemes used for the geomagnetic induction problem. As usual, a rectangular spatial mesh is defined parallel to the x and z coordinate directions. The intersections of the horizontal rows and vertical columns of the mesh are its nodes, and the mesh is assumed to be terminated at sufficient distance from the data collection sites to ensure reasonable coverage of the region influencing their data. Basically, the function V is replaced by its values v_{ij} at the nodes $\{(i, j),\ i = \overline{1, M},\ j = \overline{1, N}\}$ and a discrete approximation to (2.1) set up on the mesh.

It is important for the success of the scheme that restrictions are made on the model. Specifically, conductivity interfaces must be segments of mesh lines. With this restriction, it is convenient to discuss the model in terms of a 'basic mesh' (Madden 1973). This mesh contains only sufficient mesh lines to define boundaries, locate interfaces, and provide nodes for MT data sites and must normally be further subdivided for accuracy. A simple example of a basic mesh is shown in Fig. 1.

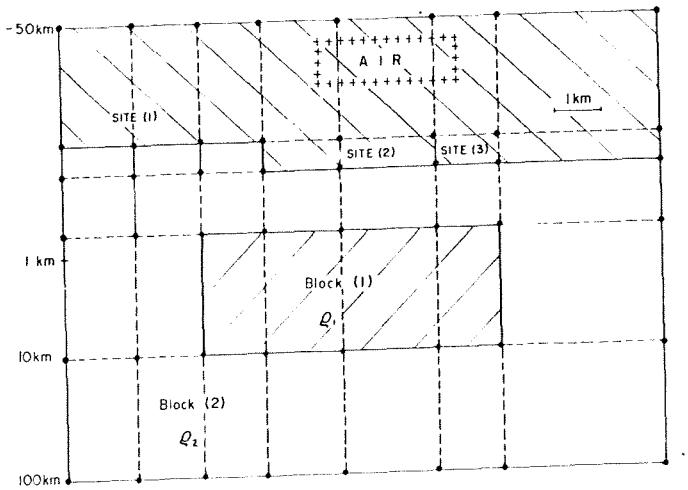

Figure 1. Simple example of a model with its basic finite difference mesh.

The most important interface is the earth–air boundary, which need not be flat, but may have approximate 2D topography. The mesh has to extend into the air for the *H*-perp polarization, but may be terminated at the highest topographic point for the *E*-perp polarization provided appropriate termination conditions are imposed (Swift 1971). In the earth, the interfaces define NB Blocks, each with resistivity ρ_k, for $k = \overline{1, NB}$. For example, in the simple model of Fig. 1, $NB = 2$ and the two Blocks have resistivities ρ_1 and ρ_2. The second 'Block' is all of the earth contained by the outer boundaries minus Block (1).

The basic mesh is normally further subdivided for an accurate finite difference scheme, so that generally, the mesh has M rows, and N columns, and each node (i, j) has an associated 'cell' (Fig. 2) with resistivity ρ_{ij}. This cell is a section of (say) the kth Block, and it is convenient in these terms to define the kth Block by the index set

$$B_k = \{(i, j) : \rho_{ij} = \rho_k\} ,$$

that is, by the set of node indices whose corresponding cell belongs to the Block.

For such a geometry, the scheme may be generated either classically using Green's Theorem on 'mesh regions' as in Varga (1962, p. 181 *ff.*), or by the network analogy as described by Swift (1967) and Madden & Swift (1969). The result is a system of linear

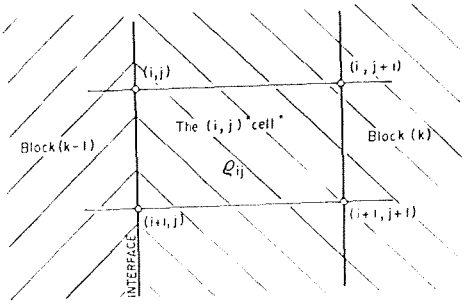

Figure 2. Diagram showing the (i, j) cell of the finite difference mesh.

equations that approximate (2.1)–(2.3).

$$A\mathbf{V} = \mathbf{S} \tag{2.4}$$

$$\mathbf{I}_x = -B\mathbf{V} \tag{2.5}$$

$$\mathbf{I}_z = -C\mathbf{V} \tag{2.6}$$

where the vector $\mathbf{V} = [v_{ij}]$ for $i = 1, M$ and $j = 1, N$ approximates V at the nodes of the extended mesh, and $\mathbf{I}_x$ and $\mathbf{I}_z$ approximate I_x and I_z at the data collection sites.

The matrix A is normal, sparse, and generally well conditioned, having only two off-diagonal bands on each side of the diagonal for the finite difference method used. The matrix decomposition for the solution of (2.4), and later equations, is very effectively accomplished by a special case of Block Gauss elimination known as the 'Greenfield algorithm' (Greenfield 1965).

Significantly, there are now two levels of approximation to real Earth structure. One is the model problem, which includes the restrictions placed by the model geometry, and consists of the general problem of model inadequacy. The other is the approximation made to the model itself by the finite difference scheme. The consequences of this second level are discussed in Section 2.3.

2.2 PARTIAL DERIVATIVES FOR INVERSION

Suppose q is a parameter of the model, which for the present case is a Block resistivity. From equation (2.4), since the source is independent of the Block resistivities, direct differentiation yields

$$A\frac{\partial \mathbf{V}}{\partial q} = -\frac{\partial A}{\partial q}\mathbf{V} \tag{2.7}$$

which may be solved for $\partial \mathbf{V}/\partial q$ once $\mathbf{V}$ is known (*cf.* Rodi 1976, for the finite element method).

Using the notation introduced in Section 2.1, if ρ_{ij} is the resistivity of the (i, j) cell, and B_k is the index set for cells in the kth Block (which has resistivity ρ_k), then

$$-\frac{\partial A}{\partial \rho_k}\mathbf{V} = \sum_{(i,j)\in B_k} \frac{\partial A}{\partial \rho_{ij}}\mathbf{V}.$$

For the finite difference scheme chosen, $(\partial A/\partial \rho_{ij})\,\mathbf{V}$ has only four non-zero terms, which can be easily calculated, making the accumulation of the vector $-(\partial A/\partial \rho_k)\,\mathbf{V}$ simple and rapid.

It follows that equations (2.4) and (2.7) may be solved by one matrix factorization and $(NB+1)$ solutions for right-hand sides, which is very much cheaper than solving $(NB+1)$ separate systems. It is this fact that justifies the claim to relatively cheap partials made in Section 1.2, and developed further in Section 2.3.

The partials for the other components follow from the direct systems

$$\frac{\partial \mathbf{I}_x}{\partial \rho_k} = -\frac{\partial B}{\partial \rho_k}\mathbf{V} - B\frac{\partial \mathbf{V}}{\partial \rho_k} \tag{2.8}$$

$$\frac{\partial \mathbf{I}_z}{\partial \rho_k} = -\frac{\partial C}{\partial \rho_k}\mathbf{V} - C\frac{\partial \mathbf{V}}{\partial \rho_k} \tag{2.9}$$

and in each case, $\partial B/\partial \rho_k$ and $\partial C/\partial \rho_k$ are sparse and straightforward to compute.

In principle, although with more complicated logic, the locations of some interfaces could be made variables as well. This extension has not been made, but it constitutes worthwhile further work.

At each site and for each frequency then, in addition to the MT ERF's, the following may be computed,

(i) E-perp to strike

$$\frac{\partial \rho_{xy}}{\partial \rho_k} = \frac{2}{\omega\mu} \operatorname{Re}\left\{\frac{\partial Z_{xy}}{\partial \rho_k} \cdot Z_{xy}^*\right\}$$

$$\frac{\partial \tan \phi_{xy}}{\partial \rho_k} = \left\{\operatorname{Im}\left(\frac{\partial Z_{xy}}{\partial \rho_k}\right) - \tan \phi_{xy} \operatorname{Re}\left(\frac{\partial Z_{xy}}{\partial \rho_k}\right)\right\} \Big/ \operatorname{Re}(Z_{xy})$$

where

$$Z_{xy} = E_x/H_y \text{ and } \frac{\partial Z_{xy}}{\partial \rho_k} = \frac{1}{H_y}\left(\frac{\partial E_x}{\partial \rho_k} - Z_{xy}\frac{\partial H_y}{\partial \rho_k}\right)$$

(ii) H-perp to strike

$$\frac{\partial \rho_{yx}}{\partial \rho_k} = \frac{2}{\omega\mu} \operatorname{Re}\left\{\frac{\partial Z_{yx}}{\partial \rho_k} \cdot Z_{yx}^*\right\}$$

$$\frac{\partial \tan \phi_{yx}}{\partial \rho_k} = \left\{\operatorname{Im}\left(\frac{\partial Z_{yx}}{\partial \rho_k}\right) - \tan \phi_{yx} \operatorname{Re}\left(\frac{\partial Z_{yx}}{\partial \rho_k}\right)\right\} \Big/ \operatorname{Re}(Z_{yx})$$

where

$$Z_{yx} = -E_y/H_x \text{ and } \frac{\partial Z_{yx}}{\partial \rho_k} = -\frac{1}{H_x}\left(\frac{\partial E_y}{\partial \rho_k} - Z_{yx}\frac{\partial H_x}{\partial \rho_k}\right).$$

The partials described are computed directly from the finite difference equations, and are the exact partials for the discrete system, but only approximations to the exact partials of the fields. Since the source is independent of the model parameters, the exact partials satisfy the following system of partial differential equations

$$L\frac{\partial V}{\partial \rho_k} = -\frac{\partial L}{\partial \rho_k} V \tag{2.10}$$

$$\frac{\partial I_x}{\partial \rho_k} = -M\frac{\partial V}{\partial \rho_k} - \frac{\partial M}{\partial \rho_k} V \tag{2.11}$$

$$\frac{\partial I_z}{\partial \rho_k} = -N\frac{\partial V}{\partial \rho_k} - \frac{\partial N}{\partial \rho_k} V \tag{2.12}$$

with homogeneous boundary conditions.

The partials of the operators L, M, and N are defined by

$$\frac{\partial M}{\partial \rho_k} = \frac{1}{Z_x'}\frac{\partial}{\partial x} \text{ where } \frac{1}{Z_x'} = \frac{\partial}{\partial \rho_k}\left(\frac{1}{Z_x}\right)$$

$$\frac{\partial N}{\partial \rho_k} = \frac{1}{Z_z'}\frac{\partial}{\partial z} \text{ where } \frac{1}{Z_z'} = \frac{\partial}{\partial \rho_k}\left(\frac{1}{Z_z}\right)$$

and

$$\frac{\partial L}{\partial \rho_k} = -\left(\frac{\partial}{\partial x}\frac{\partial M}{\partial \rho_k} + \frac{\partial}{\partial z}\frac{\partial N}{\partial \rho_k}\right) + \frac{\partial Y}{\partial \rho_k}$$

Notice that there is considerable simplification in the H-perp polarization, where Z_x and Z_z are independent of ρ_k.

Equations (2.10)–(2.12) can be solved approximately by the same finite difference method (given V from (2.7)), and the consistently discretized version of the system (2.10)–(2.13) is very similar to the system (2.7)–(2.9). In fact, for the finite difference method chosen, the two are identical. That is, (in this case) the approximate partials obtained by solving (2.10)–(2.12) by finite differences are precisely the directly evaluated partials from (2.7)–(2.9). One consequence of this identity is that for the second level of approximation (*cf.* Section 2.1) the accuracy of the finite difference scheme is the limitation in both forward evaluation, and partials computation.

2.3 THE COMPUTING COST OF MT 2D INVERSION

The forward and partials modelling methods, together with the numerical inversion methods described in Jupp & Vozoff (1974) can solve the inverse modelling problem within the limits of model inadequacy (the first level of approximation), and discretization inaccuracy (the second level).

The second level error could be reduced more or less arbitrarily provided the basic mesh could be refined by further subdivision in a more or less unlimited way. Unfortunately, apart from numerical problems, the computing cost, measured by time and storage, grows rapidly as the mesh subdivision becomes finer. In practice, therefore, the second level of approximation involves 2D inversion in an important cost/accuracy trade-off.

The program used for this paper incorporates an automatic mesh subdivision scheme due to T. R. Madden based on his measures of discretization accuracy (Madden 1973). For each frequency, the scheme ensures, by sub-division, that local discretization error is kept below some specified level. It is essential, however, that this, or any similar scheme, achieves the accuracy with the addition of as few nodes as possible, as the following timing analysis shows.

Fig. 3 describes a simple model consisting of a vertical contact with resistivities 1 and 10, and a relatively conductive overburden of resistivity 3. Apparent resistivity and phase data, computed for this model with very strict accuracy requirements, are located at three sites as shown, and comprise the 'data' for inversion. A detailed timing analysis during inversion for this model on a Univac 1106 computer indicates that for each iteration,

(i) 75 per cent of the time is taken in the matrix decomposition and solution for V and $\partial \mathrm{V}/\partial \rho_k$ ($k = \overline{1,3}$ here).
(ii) 5 per cent of the time is taken by the rest of the computation for the forward problem and partials.
(iii) 20 per cent of the time is taken by the rest of the program, which includes the inversion method, input, output, and general organization.

Because of the nature of the computations, these fractions should vary only marginally for different machines, and the large proportion of the time taken by matrix decomposition be taken as a consequence of the method.

The time for decomposition and solution for various right-hand sides depends basically on the extent of mesh subdivision, and marginally on the number of variable Blocks. As a

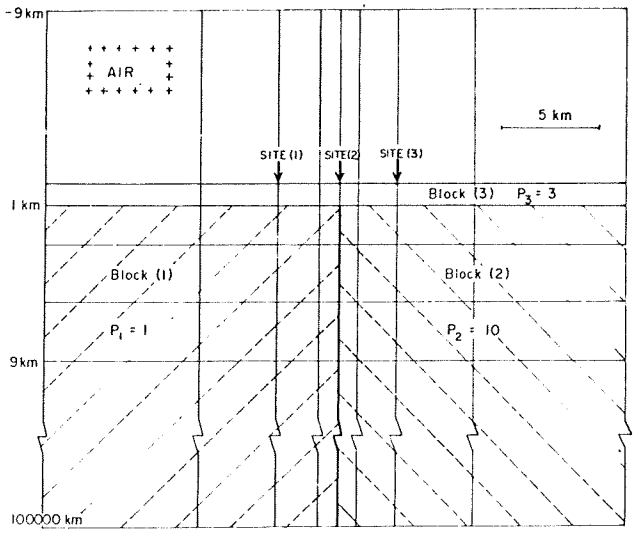

Figure 3. A simple artificial model for MT 2D inversion.

general rule, based on operation counts and pegged by actual runs, the cost per iteration has been estimated by

$$C \simeq (NB/10 + 2)F$$

where NB is the number of Blocks, and F is the time for a single forward evaluation. That is, NB must increase by about 10 Blocks to increase the cost per iteration by F, which is a consequence of the partials evaluation method of Section 2.3. Notice, however, that significant changes in NB will also increase F, since the need for further subdivision to retain the given accuracy grows.

The most significant component in the cost is F, and approximately

$$F \alpha M^3 x N x N_{\mathrm{FREQ}} \tag{2.13}$$

where M and N are the number of rows and columns of the subdivided mesh, and N_{FREQ} is the number of frequency values recorded. It is clear from this formula that as few nodes as possible should be added to achieve accuracy. For example, the simple model of Fig. 3 has a basic mesh of 6 rows and 9 columns, or 54 nodes. During inversion, to ensure local approximation to within 4 per cent, the mesh was subdivided to an average of 11 rows and 9 columns, or 99 nodes. The precise number depends on the frequency, so that over the seven frequencies used in the example, some would have more, and some less, than 99 nodes.

Both the cost increase imposed by requiring local accuracy, and its strict necessity, can be illustrated by the following artificial example. The exact model data for Fig. 3 were inverted in a very simple way by setting the three resistivities to 1 and letting them readjust. There is no problem here with misplaced interfaces, or noise on the data, and a sensitivity analysis indicates that all three parameters are very well resolved by the data.

Case (1). With no subdivision of the Basic mesh, inversion took four iterations, and 90 s Univac 1106 CP time. The final model reached was

$$(\rho_1, \rho_2, \rho_3) = (0.75, 13.4, 2.3)$$

which in view of the conditions of the problem, is greatly perturbed.

Case (2). With subdivision to 4 per cent accuracy, inversion took four iterations, and 304 s Univac 1106 CP time. The final model of

$$(\rho_1, \rho_2, \rho_3) = (1.0, 9.8, 3.2)$$

was within acceptable reach of the exact model of

$(\rho_1, \rho_2, \rho_3) = (1.0, 10.0, 3.0)$.

While the second result is still perturbed (by 4 per cent) from the exact model, even though the data are exact, the inversion took the correct path. The first result, due to poor approximation to model and partials, took a perturbed path to an incorrect solution. For more complicated examples, it is certain that valuable inversions can only be made if the cost imposed by accuracy requirements is accepted.

To summarize, given that the inversion scheme is efficient, in that the total number of iterations is kept to a minimum, accurate 2D inversions can only be obtained at respectable computing cost. This cost, although small relative to the cost of gathering data, must be justified in terms of the quality of the data, and the superior interpretation they can provide.

3 Modelling MT traverse data

3.1 DATA PRESENTATION AND MODEL PREPARATION

Effective geophysical interpretation depends on having plentiful data of high quality. In the MT method, 2D inversion may not be justified at all unless there is good data that fully samples the region being investigated. The cost of 2D inversion, as discussed in Section 2.3, itself justifies more effort in data presentation than might be given to simpler modelling.

The ERF's for MT (2D) interpretation consist of tensor rotated apparent resistivity, phase and Tipper data collected on a traverse of sites which show a consistent strike direction (*cf.* Vozoff 1972). At each site, the processed data with each sampling run plotted separately show a broad frequency dependent scatter, as is illustrated by the 906 apparent resistivity and phase values plotted in Fig. 4(a) and (b). This data is taken from a recent survey in an Australian Basin, and is typical in its noise structure. The scatter is a function of regional signal to noise properties, and must be reduced to the underlying data for effective 2D modelling.

A practical (computing) reason for reducing the data is equation (2.13), where the cost of 2D inversion is shown to be linear in the number of frequency values sampled. Moreover, the statistical benefits of removing outliers, and regional noise, from the inversion process are well known. The reduction may be made either during the data processing (*cf.* Sims, Bostik & Smith 1971; Bentley 1973), or by estimating the background noise structure of the processed data for outlier rejection, and locally averaging the overlapping data. The second method applied to the data of Fig. 4 produces Fig. 5(a) and (b) which comprise a reasonable set for input to MT 2D inversion.

The reduced data are usually collected into a 'pseudosection' (see Figs 6 and 7) for a convenient visual summary, and as input for inversion. Pseudosections were suggested by Neves (1957), and plot MT site locations on a horizontal distance scale, against frequency vertically on a $-\log f$ scale. The values of the various ERF's are filled in as a table, and separate pseudosections drawn for each polarization. For visual assessment, the pseudosection is normally contoured.

In addition to having compact, and statistically well presented data, it is essential that the initial model for 2D inversion be chosen with great care. As described in Section 1.2, the approach taken is one of model improvement, and assumes that the model being improved has prior information built into it. The sources of this information are the available geological and geophysical data for the area, and cheaper initial analyses of the MT data, which usually consist of local layered interpretation, and forward modelling.

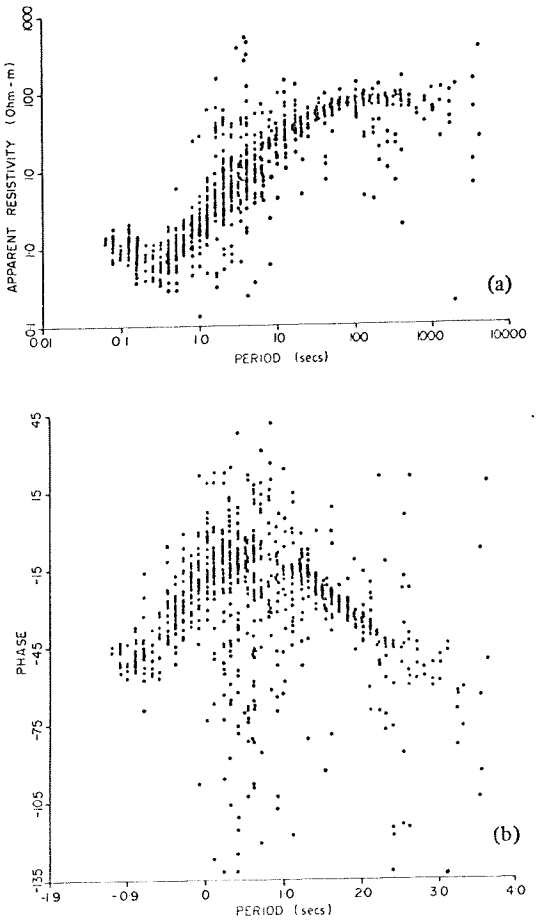

Figure 4. (a) MT apparent resistivity data from a single site showing the general frequency-dependent noise. (b) MT phase data for the same site and polarization.

An approximation to 2D structure over an MT traverse can often be made by fitting layered models separately at each site, and patching the results together as a rough resistivity section. The method described in Vozoff (1972), is further discussed in Section 3.2.

For more complex structures (Vozoff *et al.* 1975), the meaning of layered models fitted to separate polarization data becomes obscure, and their combination to form 2D sections is a process of questionable validity. However, construction of 2D starting models is a critical step in our linearized refinement modelling process. Assistance can be obtained by reference to suites of basic reference models for simple geometric figures, such as dykes, normal and reverse faults, etc., under various depths of overburden. Forward modelling, in which an appropriate example from such a suite is altered systematically, will reveal the locations of most significant discontinuities on the traverse, so that a block structure can be defined. Section 3.2 illustrates one example of the problem and a solution.

3.2 THE M3 TRAVERSE DATA

To illustrate the methods described in the paper, they are applied to some field data. The data consist of apparent resistivities for both polarizations at nine frequencies collected

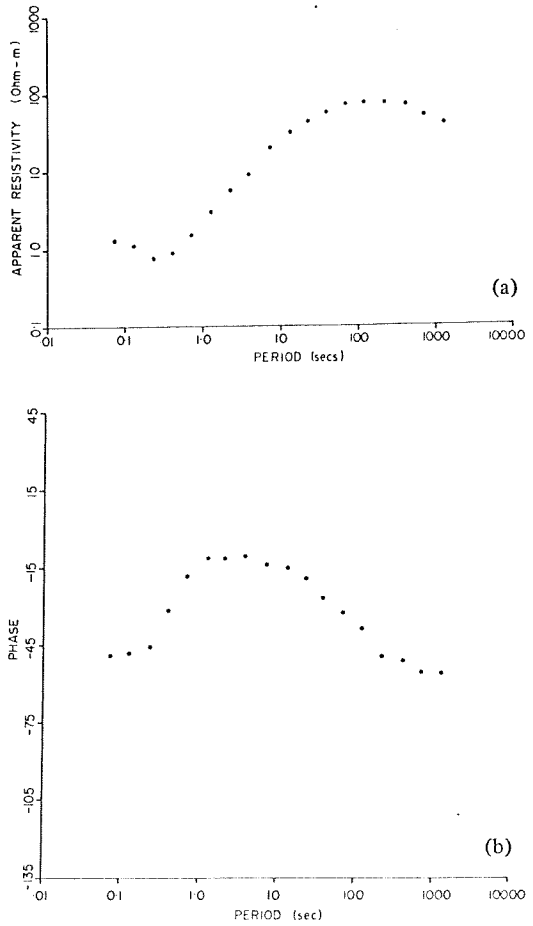

Figure 5. (a) MT apparent resistivity data of Fig. 4 reduced for inversion. (b) MT phase data of Fig. 4 reduced for inversion.

along a traverse of nine sites, and are plotted in pseudosection form in Fig. 6(a), and (b). They were collected in 1967 in Texas, and used in another context by Mitchell & Landisman (1971), but are referred to here as the M3 data.

Only the apparent resistivity data are used (as originally reported) and this, together with the gaps in the data and uncertain values, makes the data far from well-presented in the sense of Section 3.1. However, the data are typical of many field results of that vintage. Together with the basement arch structure known to exist, they illustrate the 2D inversion method well.

Earlier qualitative interpretation based on *H*-perp contoured pseudosections (Fig. 6), suggested a deep narrow conductive zone, although the missing values and uncertain data at 0.001 Hz made identification difficult. Low-frequency variations in the *E*-perp data, indicated a possible parallel resistive feature at depth.

The results of fitting layered earth models to apparent resistivities of each polarization and at each site, are presented as resistivity sections in Fig. 8(a) and (b). The two sections, one for each polarization, plot MT site locations, on the same horizontal scale as the pseudosections, against depth vertically down on a log Z scale. This exercise was relatively cheap, taking a total of 15 min Univac 1106 CP time for five modelling runs on each of the 18 data

Figure 6. (a) Pseudosection for the M3 data – *E*-perp to strike. (b) Pseudosection for the M3 data – *H*-perp to strike.

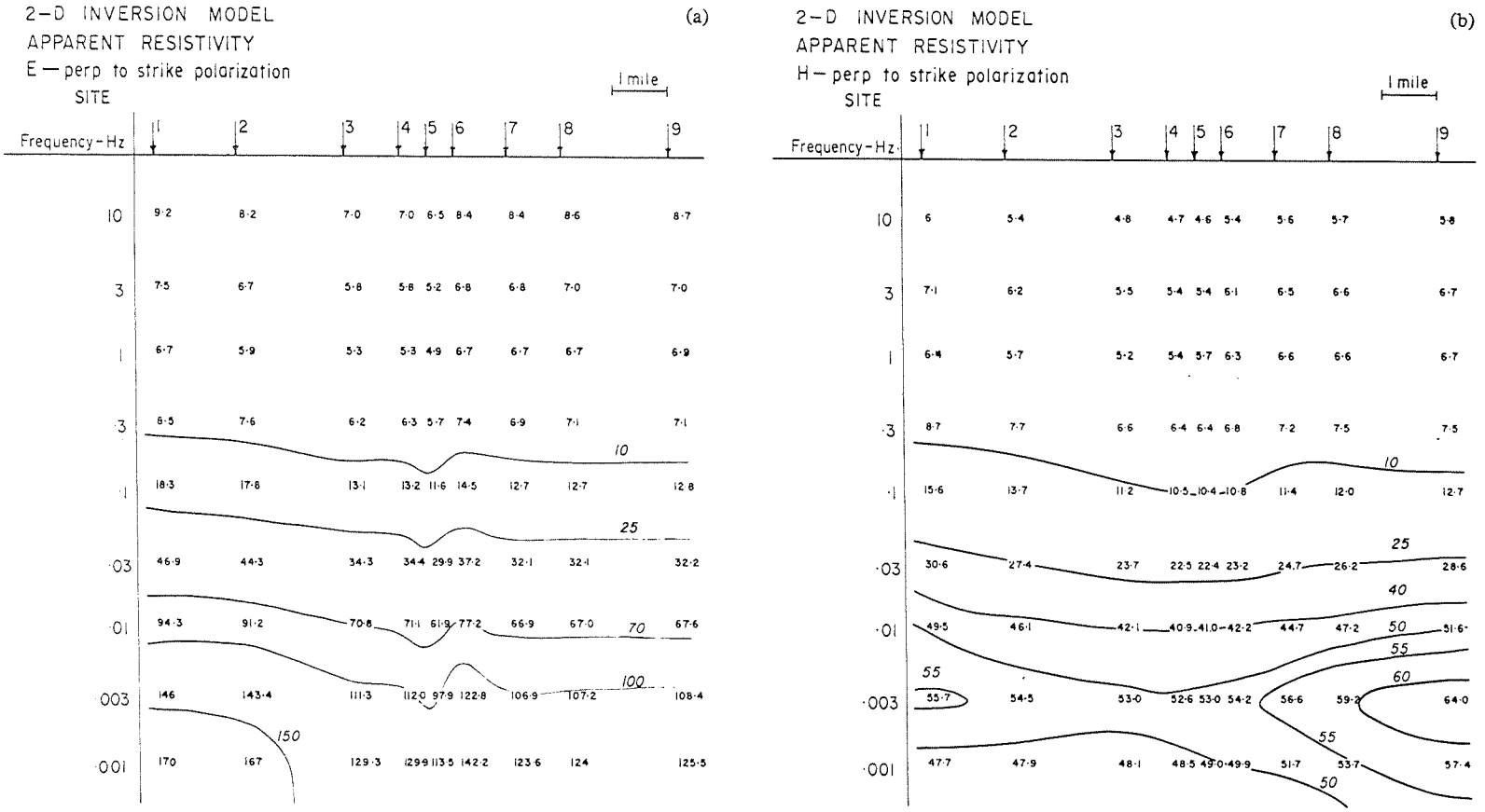

Figure 7. (a) Pseudosection for the Final Model data – *E*-perp to strike. (b) Pseudosection for the Final Model data – *H*-perp to strike.

Figure 7. (a) Pseudosection for the Final Model data – E-perp to strike. (b) Pseudosection for the Final Model data – H-perp to strike.

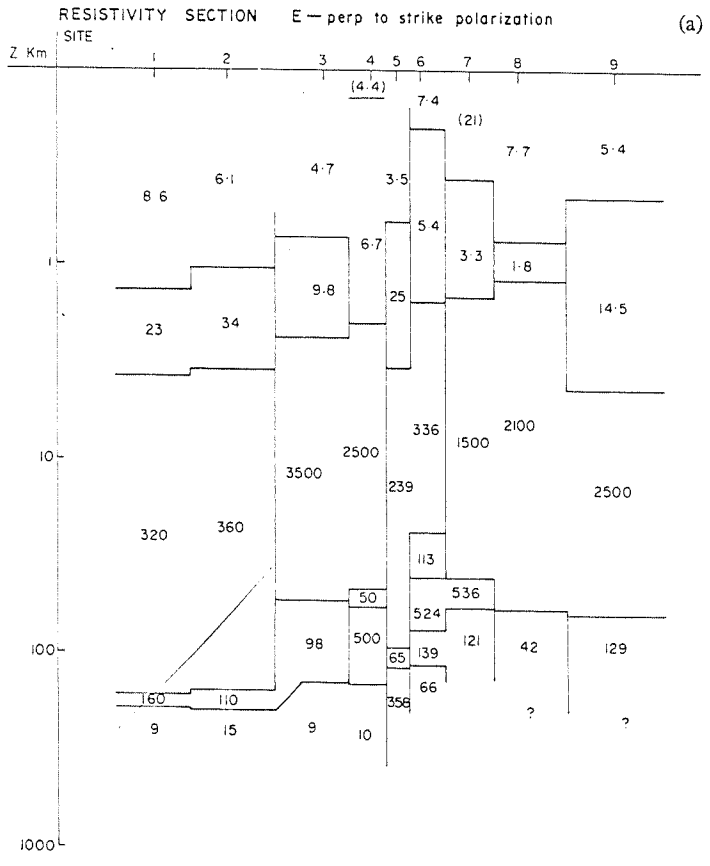

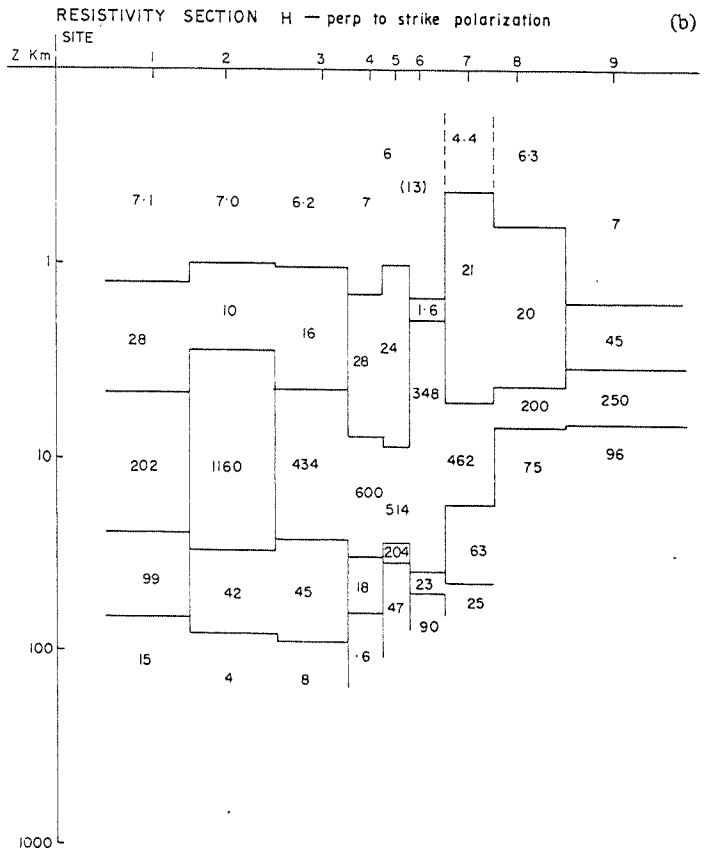

Figure 8. (a) Resistivity section inferred from layered models – E-perp to strike. (b) Resistivity section inferred from layered models – H-perp to strike.

sets. Where correlation is possible between adjacent sites the results from the local layered model inversions have been continued horizontally across the traverse for a 'regional' interpretation.

These regionalized layered inversion models are seen to form blocks from common depth intervals at adjacent sites which have approximately the same resistivities. This should always occur if site separation is sufficiently small on a traverse crossing a 2D structure. Since the two polarizations respond differently to nonlayered structures, their block patterns will differ.

Both sections of Fig. 8 show the arch, the south-dipping sediments south of the arch, a change in crustal resistivities at the arch, and other features known to occur. An objective of 2D modelling is to convert these sections to their true values. A large lateral resistivity change in the blocks of either component can only arise from a true lateral 'break' and it must be represented by a lateral block boundary in the 2D starting model. Likewise, horizontal block edges in the 2D starting model must be situated wherever large changes occur vertically in the regionalized layered models. These requirements impose severe demands when the total number of blocks as well as the numbers of rows and columns of nodes is restricted.

Only the grosser features can be accounted for. Interfaces having shallow dips may require more rows of nodes than can usually be spared. Hence shallow dips must often be approximated by horizontal surfaces, which require only a single row of nodes. Similarly, steep dips must frequently be made vertical.

The 2D starting model was constructed using the aforegoing guidelines. The excess numbers of blocks were eliminated by combining adjacent blocks having approximately the same resistivities. As will be suggested in Section 3.3, a properly constructed starting model utilizes much of the data, simplifying considerably the solution to the problem of finding block resistivities.

After some initial inversions with the *H*-perp data alone, the final model obtained using all of the data is shown as a resistivity section in Fig. 9. The model is simple, and might be improved by further addition of blocks, but confirms the general features inferred from the local layered modelling. The total fit is good at 20 per cent RMS error to all of the data consisting of apparent resistivities from all nine sites, for both polarizations, and at nine frequency values.

The mesh subdivision, in order to achieve 4 per cent local discretization error, took the basic mesh (see Section 2.1) from 12 x 18 (216 nodes) to an average of 15 x 30 (450 nodes) for each frequency, and the final run took six iterations, and 108 min of Univac 1106 CP time. This time is consistent with the rules given in Section 2.3.

The model data are plotted as pseudosections in Fig. 7(a) and (b), and contoured for comparison with Fig. 6. The model seems to be poor at 0.001 Hz in the *H*-perp polarization data, but in view of the missing data, and general uncertainty has comprised well. Clearly, for better interpretation, the missing values would be most helpful. Also, as described in Section 3.3, phase data are almost essential in any more serious interpretation.

For the purposes of this paper, the result is a good illustration of the MT 2D inversion method.

3.3 PARAMETER RESOLUTION STUDIES

An important adjunct to numerical inversion is the study of the resolution properties of the final model parameters. The approach of locally linearizing the nonlinear modelling problem at the solution was used in Jupp & Vozoff (1975) to provide measures of parameter

importance, resolution, and sensitivity to data variations. Local linearization has a number of problems and pitfalls (Anderssen 1975), but there are very informative conclusions that can be made which are stable in the sense that they remain valid for reasonable changes in the model.

Stable conclusions are made by classifying the parameters of the model as Important, or Unimportant depending on whether they correspond to relative Singular Values of the local Jacobian Matrix of partial derivatives which are above, or below, a fixed 'Threshold' value (see Jupp & Vozoff (1975) for notation and definitions). Many conclusions based on linear theory can be applied to the Important parameters, and expected to hold with respect to reasonable variations in the model (*cf.* Vozoff & Jupp 1977).

Two additional studies, based on these ideas, assume great significance for successful modelling and interpretation. The first is the study of how complex a model may be supported by a given set of data. Sensible answers to this question can be found by asking how many Important parameters can be supported and computing models with no more than this maximum number. The second study, which is illustrated with the final model for

Table 1. Parameter Importance measures, and total parameter Importance for five data situations.

Block (see Fig. 9)	Case (i) with phase	Case (ii) missing data	Case (iii) no phase	Case (iv) E_p only	Case (v) H_p only	
1	1.00	1.00	1.00	1.00	1.00	
2	1.00	1.00	1.00	1.00	1.00	
3	1.00	1.00	1.00	1.00	1.00	Surface blocks
4	1.00	1.00	1.00	1.00	1.00	
5	1.00	1.00	1.00	1.00	1.00	
6	0.98	0.98	0.98	0.97	0.98	
7	0.94	0.92	0.92	0.86	0.87	
8	0.99	0.99	0.99	0.99	0.99	
9	(0.26)	(0.20)	(0.20)	(0.16)	(0.08)	
10	0.98	0.98	0.98	(0.30)★	0.98	Conductive Dyke
11	0.92	0.91	0.91	0.91	0.75	
12	0.53†	(0.37)★	(0.39)★	(0.44)★†	(0.03)★	
13	0.93	0.90	0.91	0.91	0.93	
14	0.92	0.85	0.85	(0.03)★	0.88	
15	0.67	0.56†	0.56†	0.62	(0.06)★	
16	0.94	0.88	0.89	(0.03)★	0.78	
17	(0.49)†	(0.35)★	(0.37)★	(0.38)★	(0.13)★	
18	(0.23)	(0.19)	(0.19)	(0.06)	(0.18)	
19	0.89	0.80	0.80	0.82	0.54★†	
20	0.90	(0.24)★	(0.25)★	0.85	(0.19)★	Basement
21	0.66	(0.49)★†	(0.49)★†	0.55†	(0.18)★	
22	0.85	0.74	0.73	0.69	0.81	
23	0.74	(0.45)★†	(0.45)★†	(0.48)★†	(0.45)★†	
24	0.95	0.85	0.86	(0.47)★†	0.88	
Total Parameter Importance	19.4	17.4	17.45	15.4	15.6	

★ Significant change from column (i).
† Threshold parameter.
( ) Unresolved parameter.

the M3 data, is how parameter resolution in the final model is changed by alterations in the experimental situation.

A stable measure of parameter Importance may be defined with the notation of Jupp & Vozoff (1975) in a similar way to the damped 'error bounds' by

$$\mathbf{d} = |V|\mathbf{t}$$

where V is the parameter transformation matrix obtained from the Singular Value decomposition of the Jacobian, and the t_j's are the second order 'damping factors' described in Jupp & Vozoff (1975, Sections 2.7 and 2.8). t_j is near to 1 if the jth transformed parameter is Important, and near to zero if it Unimportant. It follows that d_i is a 'damping factor' for the ith original parameter, which is Important if d_i is close to 1 and Unimportant if it is near to zero. If d_i is near to 0.5, the parameter is said to be at the 'Threshold'.

In Table 1 the values of d_i for the 24 Blocks of Fig. 9 are presented for the following cases:

(i) All data present, and phase data as well.
(ii) The inversion situation – missing data, and no phase.
(iii) No data missing, and no phase.
(iv) E-perp data only (but with phase data).
(v) H-perp data only (but with phase data).

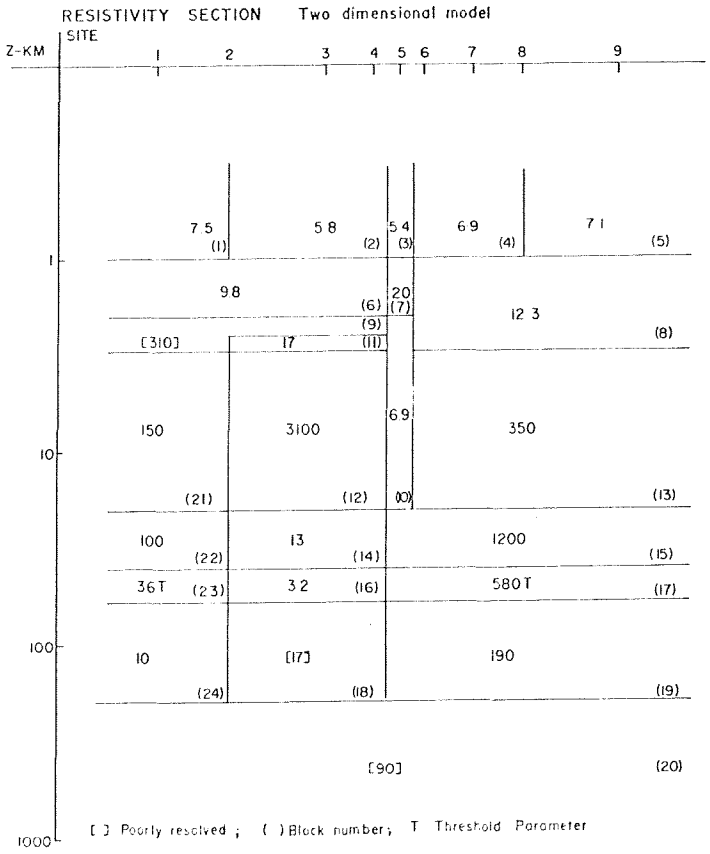

Figure 9. Resistivity section inferred from MT 2D inversion for the M3 data.

The last row of Table 1 shows the total 'number' of Important parameters as measured by the sum of the d_i's, and measures Total Parameter Importance for each case shown. This measure would be exactly the number of Important parameters if Singular Value Truncation rather than Second Order Marquardt damping were used (*cf.* Jupp & Vozoff 1975, Section 2.7).

A number of interesting conclusions are apparent.

(a) There is significant information about Blocks 12, 17, 20, 21 and 23 added by using phase data in addition to apparent resistivity data. The addition of phase data is much more significant than supplying the missing apparent resistivity data.

(b) *E*-perp and *H*-perp alone respond principally to the resistive and conductive features respectively. However, Blocks 12, 17, 21 and 23 need both sets of data to become resolved at the level chosen.

Together, these conclusions imply that phase data, which adds little to the cost of inversion should be present for effective modelling. Also, they imply that for final models, both polarization data should be used for inversion.

Conclusions

The inversion of data by modelling may be extended in a straightforward way from one-dimensional layered structure to 2D structure. When the significant increase in computing cost is justified in terms of the resulting interpretation, the methods described provide very effective interpretations of large amounts of data on a regional scale.

Since modelling consists of improving existing ideas against the data, there is much to be learnt about constructing starting models for 2D inversion from the results of simpler layered inversion. Also, in the future, a search for cheaper methods for forward modelling of complex structures would pay off when inversion methods are applied to them as they are to the finite difference method in this paper.

Acknowledgments

Support for this research was provided by the Australian Research Grants Committee and a Macquarie University Research Grant. The magnetotelluric traverse data were provided by Mobile Research and Development Corporation.

References

Anderssen, R. S., 1975. On the inversion of global electromagnetic induction data, *Phys. Earth planet. Int.*, 10, 292–298.

Anderssen, R. S., Worthington, M. H. & Cleary, J. R., 1972. Density Modelling by Monte Carlo Inversion – I. Methodology, *Geophys. J. R. astr. Soc.*, 29, 433–444.

Backus, G. E. & Gilbert, J. F., 1967. Numerical application of a formalism for geophysical inverse problems, *Geophys. J. R. astr. Soc.*, 13, 247–276.

Backus, G. E. & Gilbert, J. F., 1968. The resolving power of gross earth data, *Geophys. J. R. astr. Soc.*, 16, 169–205.

Backus, G. E. & Gilbert, J. R., 1970. Uniqueness in the inversion of inaccurate gross earth data, *Phil. Trans. R. Soc. Lond. A*, 266, 123–192.

Bentley, C. R., 1973. Error estimation in two-dimensional Magnetotelluric analyses, *Phys. Earth planet. Int.*, 7, 423–430.

Coggan, J. M., 1971. Electromagnetic and electrical modelling by the finite element method, *Geophys.*, 36, 132–155.

Glenn, W. E., Ryu, J., Ward, S. H., Peebles, W. J. & Phillips, R. J., 1973. The inversion of vertical magnetic dipole sounding data, *Geophys.*, 38, 1109–1129.

Golomb, M. & Weinberger, H. F., 1959. Optimal approximation, in *On numerical approximation*, ed. R. E. Langer, Madison, University of Wisconsin Press.

Greenfield, R. J., 1965. Two-dimensional calculations of magnetic micropulsation resonances, *PhD thesis, MIT.*

Hohmann, G. W., 1971. Electromagnetic scattering from conductors in the earth near a line source of current, *Geophys.*, **36**, 101–131.

Hohmann, G. W., 1973. Three dimensional induced polarisation and electromagnetic modelling, *43rd Annual International SEG Meeting*, Mexico City.

Inman, J. R., Ryu, J. & Ward, S. H., 1973. Resistivity inversion, *Geophys.*, **38**, 1088–1108.

Jones, F. W. & Price, A. T., 1970. The perturbations of alternating Geomagnetic Fields by conductivity anomalies, *Geophys. J. R. astr. Soc.*, **20**, 317–334.

Jones, F. W. & Thomson, D. J., 1974. A discussion of the finite difference method in computer modelling of electrical conductivity structures. A reply to the discussion by Williamson, Hewlett and Tammemagi, *Geophys. J. R. astr. Soc.*, **37**, 537–544.

Jupp, D. L. B. & Vozoff, K., 1975. Stable iterative methods for the inversion of geophysical data, *Geophys, J. R. astr. Soc.*, **42**, 957–976.

Ku, C. C., 1976. Numerical Inverse Magnetotelluric problems, *Geophys.*, **41**, 276–286.

Lanczos, C., 1960. *Linear differential operators*, D. Van Nostrand, London.

Lee, T., 1975. An integral equation and its solution for some two-and-three dimensional problems in resistivity and induced polarisation. *Geophys. J. R. astr. Soc.*, **42**, 81–95.

Lilley, F. E. M., 1974. Analysis of the geomagnetic induction tensor, *Phys. Earth planet. Int.*, **8**, 301–316.

Madden, T. R. & Swift, C. M., 1969. Magnetotelluric studies of the electrical conductivity structure of the crust and upper mantle, in AGU Monograph 13, *The Earth's Crust and Upper Mantle*, p. 469–479.

Madden, T. R., 1972. Transmission systems and network analogies to geophysical forward and inverse problems, *Tech. Rept. No. 72–3*, Department of Earth and Planetary Sciences, MIT.

Madden, T. R., 1973. *Instruction Manual for EMCDC and EMUVC (EMCAL)*, Exploration Aids, Inc., Needham, Massachusetts.

Marquardt, D. W., 1970. Generalised inverses, Ridge Regression, biased linear estimation, and non linear estimation, *Technometrics*, **12**, 591–612.

Mitchell, B. J. & Landisman, M., 1971. Electrical and seismic properties of the Earth's crust in the southwestern Great Plains of the USA, *Geophys.*, **36**, 363–381.

Neves, A. S., 1957. The Magnetotelluric method in two dimensional structures, *PhD thesis, Dept. of Geology and Geophysics, MIT.*

Parkinson, W. D., 1959. Direction of rapid geomagnetic fluctuations, *Geophys. J. R. astr. Soc.*, **2**, 1–14.

Patrick, F. W. & Bostick, F. X., 1969. Magnetotelluric modelling techniques, EERL, Texas University, *Tech. Report No. 59.*

Praus, O., 1975. Numerical and analogue modelling of induction effects in laterally non-uniform conductors, *Phys. Earth planet, Int.*, **10**, 262–270.

Rodi, W. L., 1976. A technique for improving the accuracy of finite element solutions for MT data, *Geophys. J. R. astr. Soc.*, **44**, 483–506.

Sims, W. E., Bostick, F. X. & Smith, H. W., 1971. The estimation of magnetotelluric impedance tensor elements from measured data, *Geophys.*, **36**, 938–942.

Swift, C. M., 1967. A Magnetotelluric investigation of an electrical conductivity anomaly in the southwestern United States, *PhD thesis, MIT.*

Swift, C. M., 1971. Theoretical Magnetotelluric and Turam response from two-dimensional inhomogeneities, *Geophys.*, **36**, 38–52.

Varga, R. S., 1962. *Matrix iterative analysis*, Prentice-Hall, New Jersey.

Vozoff, K., 1972. The magnetotelluric method in the exploration of sedimentary basins, *Geophys.*, **37**, 98–141.

Vozoff, K., Kerr, D., Moore, R. F., Jupp, D. L. & Lewis, R. G., 1975. Murray basin magnetotelluric study, *J. geol. Soc. Australia*, **22**, 361–375.

Vozoff, K. & Jupp, D. L. B., 1975. Joint inversion of Geophysical data, *Geophys. J. R. astr. Soc.*, **42**, 977–991.

Vozoff, K. & Jupp, D. L. B., 1977. Effective Search for a buried layer: an approach to experimental design in geophysics, *Bull. A.S.E.G.*, in press.

Weidelt, P., 1975. Inversion of two-dimensional conductivity structures, *Phys. Earth planet. Int.*, **10**, 282–291.

Williamson, K., Hewlett, C. & Tammemagi, H. Y., 1974. Computer modelling of electrical conductivity structures, *Geophys. J. R. astr. Soc.*, **37**, 533–536.

Wu, F. T., 1968. The inverse problem of Magnetotelluric sounding, *Geophys.*, **33**, 972–979.